

# UG376: OCCUPANCY-EXP-EVB User's Guide

The Silicon Labs' OCCUPANCY-EXP-EVB evaluation kit is an expansion board for EFM32 Starter Kits (STKs). The evaluation kit is intended for demonstration and evaluation of an occupancy sensing and ambient light sensing system with Silicon Labs MCU and sensor products.

**Note:** Software examples are provided for the EFM32 Pearl Gecko12 Starter Kit SLSTK3402A (sold separately).

## KEY FEATURES

- Quick start demonstration of occupancy sensing and ambient light measurements.
- Discusses the theory of operation and implementation considerations of occupancy sensing and ambient light sensing systems.
- Provides performance summary and testing methodologies for evaluating systems.
- Compatible with SLSTK3402A EFM32 PG12 starter kit.

## SOFTWARE FEATURES

- Firmware Code
- Energy Profiler
- PIR GUI



# Table of Contents

<b>1. Introduction . . . . .</b>	<b>3</b>
1.1 Getting Started . . . . .	3
<b>2. Kit Block Diagram . . . . .</b>	<b>4</b>
<b>3. Kit Hardware Layout . . . . .</b>	<b>5</b>
<b>4. Theory of Operation . . . . .</b>	<b>6</b>
4.1 PIR Sensor & Optical Design . . . . .	7
4.2 Analog Signal Amplification and Filtering . . . . .	9
4.3 Signal Digitization and Detection . . . . .	11
4.4 Additional Occupancy Sensing Considerations . . . . .	12
4.4.1 Power Supply Design . . . . .	12
4.4.2 Performance Improvements . . . . .	12
4.5 Ambient Light Sensing . . . . .	13
<b>5. Test Results . . . . .</b>	<b>14</b>
5.1 Occupancy Sensing . . . . .	14
5.1.1 Detection Sensitivity. . . . .	14
5.1.2 Noise Immunity . . . . .	14
5.1.3 Power Measurement . . . . .	15
5.2 Ambient Light Sensing . . . . .	15
5.2.1 Accuracy . . . . .	15
5.2.2 Power Measurement . . . . .	16
<b>6. Hardware Details . . . . .</b>	<b>17</b>
6.1 Schematics . . . . .	17
6.2 Bill of Materials . . . . .	17
6.3 Assembly Drawings . . . . .	17
6.4 Gerber Files . . . . .	17
6.5 Expansion Header. . . . .	18
<b>7. Software Details . . . . .</b>	<b>20</b>
7.1 Importing the Firmware Example . . . . .	20
7.2 PIR GUI Details. . . . .	21
<b>8. Kit Revision History and Errata . . . . .</b>	<b>22</b>
8.1 Revision History . . . . .	22
8.2 Errata . . . . .	22
<b>9. Revision History . . . . .</b>	<b>23</b>

## 1. Introduction

The Silicon Labs' OCCUPANCY-EXP-EVB evaluation kit is an expansion board for EFM32 Starter Kits (STKs). The evaluation kit is intended for demonstration and evaluation of an occupancy sensing and ambient light sensing system with Silicon Labs MCU and sensor products.

**Note:** Software examples are provided for the EFM32 Pearl Gecko12 Starter Kit SLSTK3402A (sold separately).

### 1.1 Getting Started

1. Connect the OCCUPANCY-EXP-EB board to the SLSTK3402A EFM32 PG12 Starter Kit.
2. Launch the OCCUPANCY-EXP-EVB example code from Simplicity Studio. Follow the instructions in [7.1 Importing the Firmware Example](#)
3. Select a demo on the LCD screen by navigating with the PB0 button.
4. For the PIR demo, the LED will light up for motion events. The PIR demo will also stream samples to the PIR GUI tool for waveform visualization.

For test setup, follow the description in [5.1.1 Detection Sensitivity](#). The firmware is set to assert the motion signal for 5 seconds after motion is detected.

5. For the ambient light demo, the ambient light level in lux will be reported on the LCD.

## 2. Kit Block Diagram

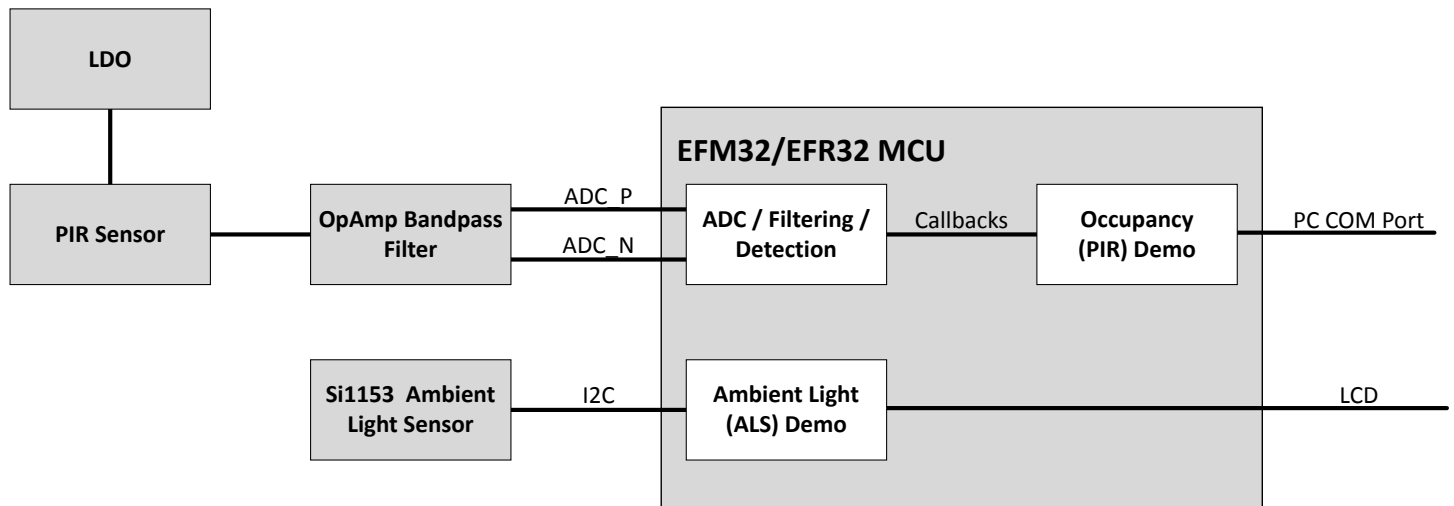


Figure 2.1. Occupancy Sensing and System Block Diagram

### 3. Kit Hardware Layout

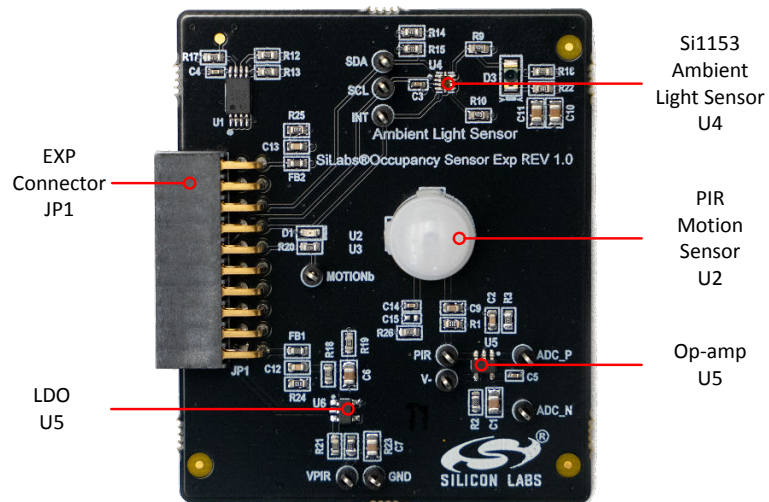


Figure 3.1. Kit Hardware Layout

## 4. Theory of Operation

From offices to the home, connected energy-efficient systems can generate energy savings and personalize work and living spaces. Lighting systems can benefit from occupancy sensors, which can turn off lights when not needed, and ambient light sensors which can adjust the ambient light level based on available light. These systems need to be robust and low power.

Using Silicon Labs EFM32/EFR32 MCUs and Si1153 ambient light sensor, this evaluation kit demonstrates an occupancy sensing and ambient light sensing solution.

At a glance, the occupancy sensing circuit is implemented by a low-cost analog PIR sensor with an op-amp based bandpass filter optimized for low power and high sensitivity. The strength of this solution comes in the signal processing implemented on the MCU. The MCU implements a software digital filter to further reduce noise and a configurable motion detector. The MCU stays in EM2 sleep mode during sampling and only wakes up for motion events and periodically to update the filter. This design was tested to be robust for occupancy detection and immune against electronic noise, ambient lighting and temperature changes.

The ambient light sensing circuit is based on the Si1153 digital optical proximity and ambient light sensor. The Si1153 has an integrated photodiode for light measurements and can be configured for autonomous or directed operation. Ambient light levels, as perceived by humans, are estimated by using both integrated photodiodes. Additionally, optical flicker rejection is reduced through an efficient ADC sampling method.

This user guide discusses the theory of operation and test results of both the occupancy sensing and ambient light sensing solutions.

## 4.1 PIR Sensor & Optical Design

The pyroelectric infrared (PIR) sensor is used in many occupancy-sensing systems. The sensor converts fluctuations in incoming infrared (IR) radiation into an analog voltage. PIR sensors consist of an optical filter, pyroelectric elements, and a buffer. The figure below shows a circuit representation of the sensor. The optical filter only allows IR radiation to enter the sensor. The elements are connected in series in opposite polarity to generate differential sensing. If a common mode IR disturbance occurs, such as a change in the ambient temperature, both elements generate voltages that oppose each other and cancel.

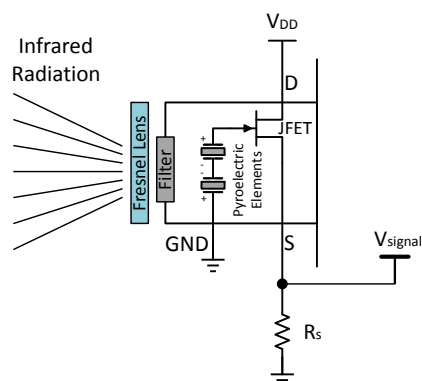


**Figure 4.1. PIR Sensors Have an Optical Filter, Pyroelectric Elements and a Buffer**

The output of the pyroelectric elements is buffered with a JFET source follower because of the high-output impedance of the pyroelectric elements. The JFET bias current is set by the  $R_s$  resistor, which affects the sensor sensitivity, noise, and current consumption. The output signal is taken at the source terminal of the sensor.

An illustration of the  $V_{\text{SIGNAL}}$  output signal is shown in the right half of the figure below moving across the field of view of the sensor. The DC value is typically between 0.5 – 1 V and the signal amplitude is in the range of 10 s of  $\mu\text{V}$  to mV. The amplitude depends on the object's distance, size, temperature and speed. The width of pulse is related to the speed of the object and the size of the detection zones.

An important consideration for PIR sensor is power supply rejection. The power supply rejection at the source output is limited to ~20 dB attenuation of variation at the drain input due to the internal source follower circuit. To achieve a low noise signal, proper power supply design must be considered, which is discussed in [4.4.1 Power Supply Design](#).

The other major component in the optical design is a Fresnel lens placed in front of the PIR sensor. The lens increases the sensitivity of the system by focusing the field of view into detection zones and is essential for the proper functioning of a PIR system. The lens is comprised of multiple lenses at different angles to create the detection zones as shown in the figure below. The lens design will set the detection pattern and field of view of the application. Examples of optimizations are narrow or wide field of views or detection patterns meant to cover wide space from overhead. The end application should inform the design of the lens and should not be left unoptimized.

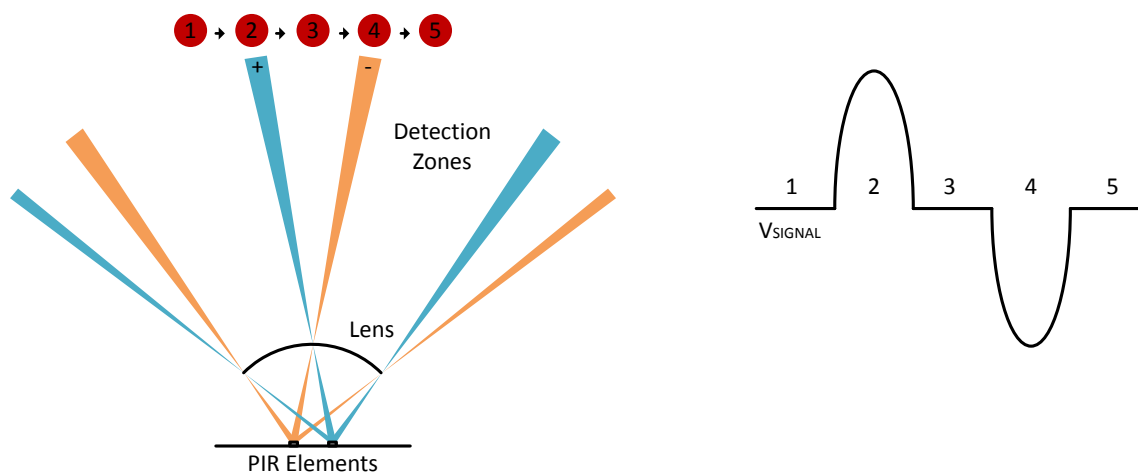


**Figure 4.2. PIR Fresnel Lens Focus the IR to Increase Range and are Made of Multiple Lenses to Create Detection Zones**

The left-hand side of the figure above shows the pyroelectric elements interacting with a lens array that consists of three lenses. The lens focuses the light onto the elements. The lens at different angles causes the three detection zones per element. Consider a person walking across the detection pattern, as indicated by the objects at the top. As they approach position 2, the heat is picked up by the

positive element, causing a rise in the output voltage. As they walk past position 4, the negative element picks up the heat while the positive element sees nothing and the output goes negative.



## 4.2 Analog Signal Amplification and Filtering

The analog signal amplification and filtering is shown in the figure below. The amplification scales the signal, so that the amplitude is large enough to interface with the detector. The bandpass filtering removes high-frequency noise and low-frequency drift that are not associated with motion.

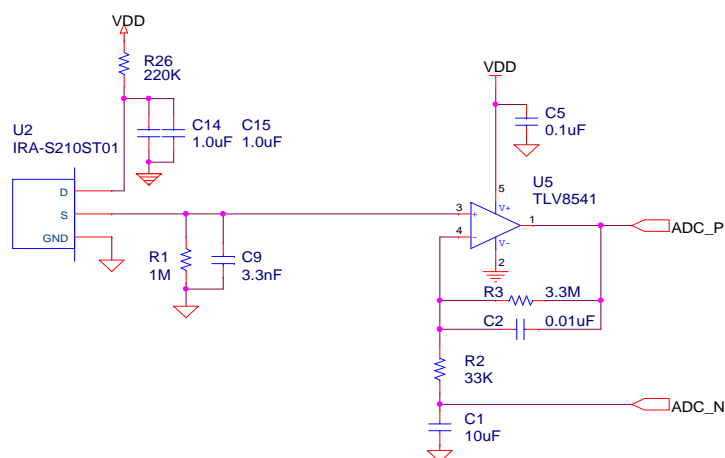


**Figure 4.3. Simplified Schematic Showing Amplification and Bandpass Filtering**

The PIR signal initially comes from the source terminal of U2. The bias current of the PIR sensor is set by R1. Maximum optical sensitivity is obtained around 10-100 kΩ, however these source resistances result in high bias current which is not suitable for low power designs. The bias current can be calculated by dividing the nominal source voltage specified in the sensor datasheet by the source resistance. The source resistor was set at 1 MΩ to decrease the bias current to under 1 μA. The increased source resistance was measured on a typical part to result in -30% sensitivity, which is an acceptable tradeoff for the reduced bias current.

The amplification is provided by the non-inverting op-amp circuit of U5. The non-inverting circuit has high input impedance and does not require another voltage source to bias the output. An inverting architecture would need a high-impedance resistor divider and sizable decoupling capacitor to form the virtual ground voltage and avoid coupling power rail variation. The passband gain and filter cutoff frequencies are calculated below. The low-cutoff frequency strongly affects how the system responds to motion. A lower-cutoff frequency suppresses slow motion peaks less increasing system sensitivity to slow motion, but also allows more flicker noise and drift effects into the system. Typical designs might use a low-cutoff frequency between 0.1 – 1 Hz. A caution on very low-cutoff frequencies is that it introduces a long RC into the system which can take a long time to settle and can require large resistances and capacitances which have implications on size and cost. The high-cutoff frequency can be adjusted to control high-frequency noise. However, be careful to avoid reducing the passband gain.

$$A_v = 1 + \frac{R3}{R2} = 101, f_{c,low} = \frac{1}{2\pi \times R2 \times C1} = 0.48 \text{ Hz}, f_{c,high} = \frac{1}{2\pi \times R3 \times C2} = 4.82 \text{ Hz}$$

**Equation 1: Hand Calculations for Filter Passband Gain and Cutoff Frequencies**

The relevant characteristics of the op-amp are its current consumption and voltage noise. For a low-power system, sub μA level op-amps can be used. In exchange for the low current consumption, these op-amps will have reduced gain-bandwidth or slew rate considerations. Aim to have the gain-bandwidth at least a decade above the circuit gain-bandwidth to avoid non-ideal op-amp effects. Other analog designs will go to higher passband gain and split the system gain into multiple stages to avoid the gain-bandwidth limitation. This design demonstrates that the higher gain is not necessary and that a second op-amp stage can be eliminated.

This design uses an external op-amp to get to the lowest system current. The EFM32 MCUs have internal op-amps that can also be used to replace the external op-amp. This reduces BOM cost and board space as all amplification and detection can be performed inside the MCU. The firmware supports the internal op-amp configuration. This requires use of the op-amp main ports.

The differential input to the ADC is taken at the main bandpass output and between R2 and C1 which are the components which set the low-frequency cutoff. The differential voltage between these nodes eliminates the unity gain low-frequency response of the non-inverting amplifier, which is important to remove flow-frequency flicker noise. The magnitude of the bandpass filter is shown in the figure below. The passband gain is slightly less than the hand calculation voltage gain due to the proximity of the two poles.

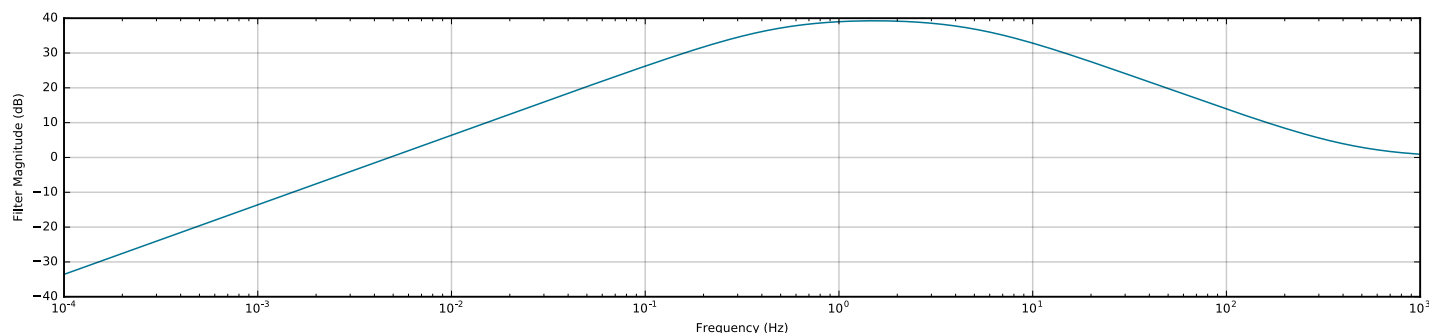


**Figure 4.4. Bandpass Characteristic of ADC\_P – ADC\_N**

The start up time of this circuit depends on the time constant  $R3 * C1$ . During start-up, the op-amp saturates at the positive power rail while the  $C1$  capacitor charges. Due to the high resistance and capacitance for large gain and low frequency cutoff, this can lead to tens of seconds for start up time.

Some designs place diodes across the feedback network of the non-inverting amplifier to short the feedback resistor  $R3$  during start up when a large forward voltage occurs across the diode. While this is effective in reducing the start-up time, the parasitic parallel resistance and saturation current cause a reduction in the passband gain, even at low voltage. This effect was simulated and measured to cause approximately a 30% loss in passband gain with a 3.3 M $\Omega$  feedback resistor while using a low saturation current diode. Furthermore, this can only be applied to the first stage, as the second stage will consistently exceed the forward voltage due to the high gain, resulting in gain attenuation.

This design eliminates the feedback diodes to restore the sensitivity. The start up time is equivalent to start up times on designs which do not have diodes on their second stage and better than two stage designs with no diodes.

### 4.3 Signal Digitization and Detection

The motion signal is digitized by an ADC and analyzed by a detection algorithm with adaptive thresholds. The adaptive thresholds are based upon a software low passed version of the motion signal to provide additional drift removal. The ADC sampling operates fully autonomously in EM2 deep sleep allowing for low-power operation while the hardware thresholds allow for immediate MCU wakeup upon detection. A block diagram of the firmware operation is shown in the figure below. The firmware is provided as a demonstration and the operation can be easily modified or augmented if other optimizations are desired.

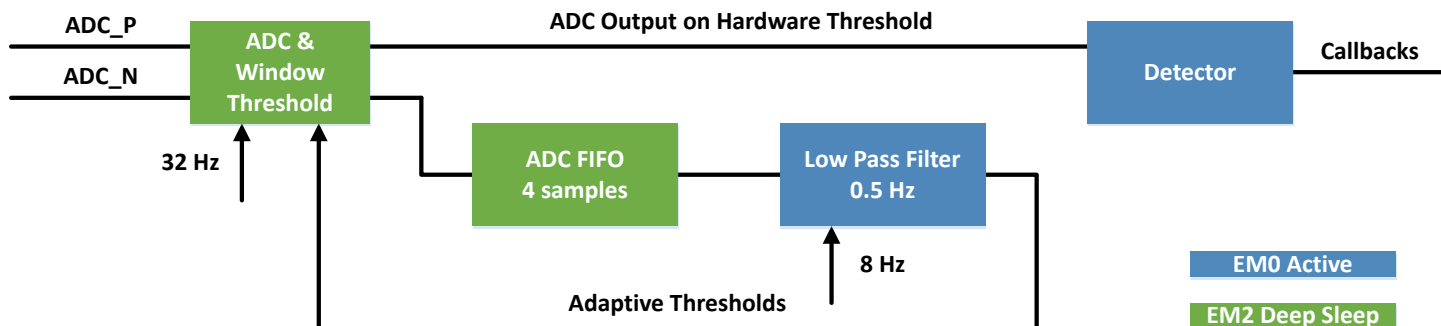


Figure 4.5. Firmware Block Diagram

The ADC is operated differentially to cancel out the low-frequency drift common on the ADC\_P and ADC\_N inputs. The inputs are routed through the analog APORT buses allowing for flexible pin selection for the inputs. The sampling clock is driven by the CRYOTIMER block connected through the peripheral reflex system (PRS) to trigger the ADC sampling. The ADC has software programmable thresholds that can be used to interrupt the MCU. Both the threshold interrupt and ADC FIFO interrupt are enabled, so that the host can be informed when detection has occurred or to update the thresholds. The batching of samples in the ADC FIFO prior to the low-pass filter reduces the wakeup frequency of the MCU for the low-pass filter and correspondingly the current consumption.

The ADC is operated on the 1.25 V internal reference and at 16-bit resolution. This configuration gives 19.1  $\mu$ V PIR sensor input referred resolution.

The detector is a window comparator centered around the output of the software low-pass filter. By adjusting the center of the window, the detector sensitivity to low-frequency drift is further reduced. The detector threshold determines motion sensitivity and noise sensitivity of the system which can be translated back to detection distance and false positive rate. The motion sensitivity is  $\text{Threshold} / H_{\text{system}}(j\omega)$  where  $H_{\text{system}}(j\omega)$  is the optical input to ADC output transfer function.

To increase the motion sensitivity and detection distance, either decrease the threshold or increase the system sensitivity in optical, sensor, or analog blocks. The detection level to noise ratio is  $\text{Threshold} / \text{Noise}_{\text{system}}$  where  $\text{Noise}_{\text{system}}$  is the combination of all noise sources referred to the output. If the threshold is too low, false positives occur, but if it is too high, the motion sensitivity is reduced. As a rule of thumb, keep the threshold at a minimum of 5 times the RMS noise of the system. Adjusting the threshold is a trade off between motion sensitivity and noise sensitivity, but to increase the detection distance at a set false positive rate, either the system gain must be increased, or the system noise must be reduced.

The low-pass filter that feeds the detector is implemented as a discrete time first order IIR low-pass filter. The filtered output is fed back to the ADC to generate the upper and lower thresholds of a window detector. This helps to eliminate any remaining drift in the signal. The filter cutoff frequency is configurable in software and was set at 0.5 Hz to match the analog cutoff frequency.

## 4.4 Additional Occupancy Sensing Considerations

### 4.4.1 Power Supply Design

The power supply rejection of the PIR circuit is limited by the PIR sensor JFET source follower to approximately 20 dB. Transients and noise on the power supply can couple into the system and cause false detections. The power rail should be regulated and filtered to minimize disturbances.

The PIR sensor supply should be regulated with a separate LDO that has good line regulation. Minimize power rail series resistance to reduce the voltage droop during heavy load current.

RC filtering should be used at the drain of the PIR sensor to reduce the power supply noise coupling into the signal. The power supply filter corner should be lower than the signal lower frequency corner. To achieve the low frequency corner, the series resistance can be increased to keep the capacitance small. The series resistance causes a reduction in the PIR  $V_{DS}$ . For this design, reducing the  $V_{DS}$  below 1.5 V was found to start to affect the signal gain. From this  $V_{DS,min}$ , combined with  $V_S$  and  $R_S$  the maximum drain resistance to avoid signal gain loss can be computed.

If a disturbance is known ahead of time, such as a wireless transmission, the detection can be temporarily disabled during the event to prevent false detection. The detection threshold can be increased to reduce the transient sensitivity. However, this also reduces the motion sensitivity.

### 4.4.2 Performance Improvements

Applications may want to optimize this system for a specific system performance. This section discusses modifications to optimize for high sensitivity and low power.

For high-sensitivity long-range detection performance, the system needs to maximize the system gain and minimize noise. Starting at the sensor, look for PIR sensors with high responsivity and low noise. Set the bias resistance closer to the manufacturer's recommended value to avoid the sensitivity loss associated with the low-bias current used in this design. Field of view and detection distance can be traded off in the Fresnel lens. Multiple PIR sensors can be used to restore the system field of view. Larger Fresnel lens arrays can be mounted further away from the sensor and focus IR from further distances. The low-frequency corner of the filter can be reduced to broaden the energy captured. Most designs will not go below 0.1 - 0.25 Hz. The analog gain can be increased but may need to be split across a second stage. Reducing the system noise will allow decreasing the motion threshold at the same false detection rate.

For low-power designs, the current consumption is mainly in the EM2 sleep current and software processing. The EM2 sleep current can be reduced further through disabling RAM retention. Decreasing the adaptive threshold refresh rate will reduce the EM0 current consumption. As an alternative to the software-based detection, the analog comparators on the EFM32 can be used as an analog window comparator. The comparators can operate at as low as 50 nA current consumption.

## 4.5 Ambient Light Sensing

Ambient light sensors measure light in terms of its perceived brightness to the human eye. The scientific field of optics related to perceived human brightness is known as photometry. The human eye has a weighed response to visible light known as the photopic response, as shown in the figure below.

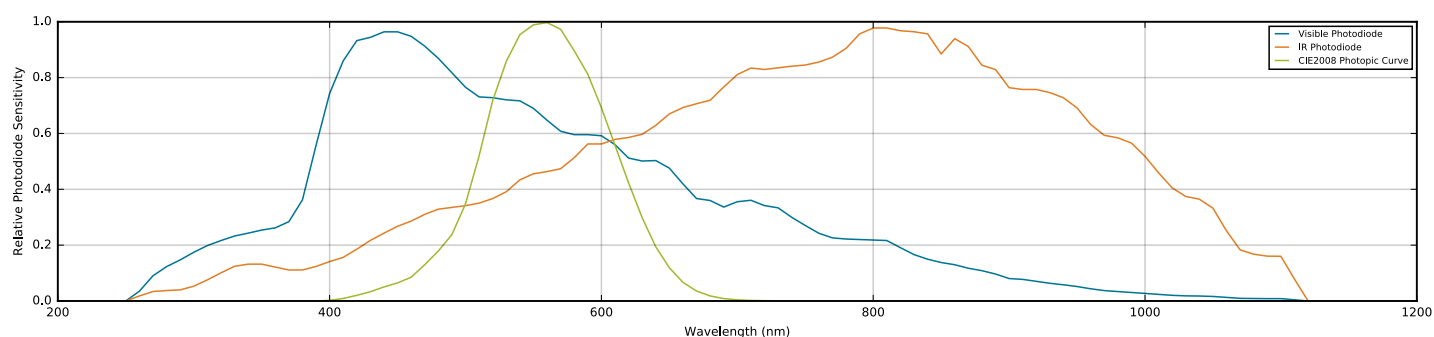


**Figure 4.6. Relative Sensitivity Curves for the CIE Photopic Curve and the Si1153 Visible and IR Photodiodes**

The amount of light incident on a surface per unit area is known as illuminance. The unit of illuminance is lux. Typical illuminance levels for several conditions are listed in the table below as a reference. The important parameters of an ambient light sensor are its accuracy, light source variation, and current consumption.

**Table 4.1. Typical Illuminance Levels**

Condition	Illumination (lux)
Nighttime	< 1
Indoor Lighting	100 - 500
Overcast Day	1000
Full Daylight	10,000 – 100,000

The Si1153 has two photodiode responses, a visible photodiode which peaks near 450 nm and an infrared (IR) photodiode that peaks near 800 nm. These two measurements are combined to create equations that estimate the illuminance. The equations depend on estimations of the spectral output of the light and the coefficients used depend on the type of light characterized by the IR to visible ratio. The following equations were empirically derived by testing multiple incandescent, fluorescent, halogen and LED bulbs. These equations are derived for broadband sources, and should not be used for accurate illuminance measurements of narrow band or colored sources without additional characterization.

Condition	Lux Equation
$1 < \frac{IR}{Visible}$	$lux = 0.0938 \times Visible + -0.0131 \times IR$
$0.7 < \frac{IR}{Visible} < 1$	$lux = 0.1842 \times Visible + -0.0822 \times IR$
$\frac{IR}{Visible} < 0.7$	$lux = -0.2140 \times Visible + 0.5302 \times IR$

Ambient light sensors often have functionality to reject optical flickering of the lights at the power mains frequencies and its harmonics. In older certain lighting, the optical flickering can be as much as 20% of the average intensity.

Rejection of the optical flicker is accomplished by integrating over 100 ms, which provides both 50 and 60 Hz rejection. In this implementation, the Si1153 is commanded to perform 16 samples of 24.4  $\mu$ s evenly spaced in 100 ms. These samples are averaged to form the final ADC result. This sampling approach provides effective optical flicker rejection while also efficiently conserving power.

## 5. Test Results

### 5.1 Occupancy Sensing

#### 5.1.1 Detection Sensitivity

The detection distance was tested at various distances. The board was mounted on the wall, 2 m above the floor. Testing was only performed at the 0° angle. The test consisted of an initial idle time of 30 seconds, walking in alternate directions 5 times at 15 second intervals, and a final 30 second idle time. The direction of movement was across the field of view of the sensor. Detection is counted if the system detects motion on any of walks. False detection is counted if the system detects motion at any point during either of the idle periods.

The software was configured with its default configuration of 32 Hz ADC sampling and 1024 lsb window size.

Lens Type	Detection Distance	False Detections
IML-0685 Wide Angle	30 ft	None
IML-0588 Ceiling Type	25 ft	None

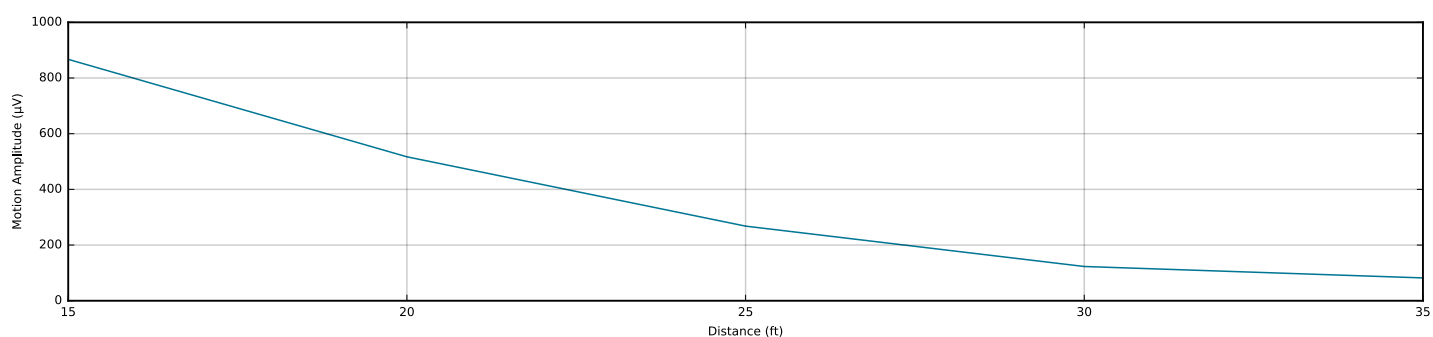


Figure 5.1. Typical Motion Amplitude Over Distance

#### 5.1.2 Noise Immunity

The false alarm rate and noise immunity of the system was tested through several approaches detailed below. The system was found to be robust against ambient change, temperature changes and vibration.

Table 5.1. False Alarm Summary

Test	False Detections
24-hour Ambient Light & Temperature Test	None
Mechanical Shock Test	None
Hot Air Test	None

The tests were performed without a person in the field of view of the sensor. Any motion detection would be counted as a false detection.

The 24-hour ambient test was performed by leaving the system in an empty room facing a window with sunlight exposure. The system was exposed to daylight variation and temperature variation over the course of the day and digitally monitored for false detections. This long duration test also verified that the electronic noise of the circuit would not trigger a false positive.

The mechanical shock test was performed by mounting the detector on a table and hitting the table next to the detector and verifying there were no false detections.

The hot air test exposed the detector to turbulent hot air across the face of the detector. The detector was monitored for false detections when the hot air was turned on and off.

### 5.1.3 Power Measurement

The current consumption of the system was measured using the Advanced Energy Monitoring (AEM) tool included in the Starter Kit hardware and Simplicity Studio. This tool allows for real time monitoring of current consumption with 0.1  $\mu\text{A}$  resolution at 6.3 ksps. Average current was measured over 30 s to account for the pulsed nature of the software. All current consumption through the VMCU power rail is measured which includes the MCU, LDO, op-amp, PIR sensor. The indicator LED is not included in the current.

The 'PIR LCD OFF' demo was used for the power measurement and will directly give the total system current. Block level currents were measured by disabling individual blocks in firmware. The LDO / Op-Amp / PIR Sensor measurement was performed by placing the MCU in EM4 Shutoff for baseline and measuring the current with and without the expander board attached.

Block	Current Consumption
LDO / Op-amp / PIR Sensor	1.4 $\mu\text{A}$
EFM32 MCU EM2	3.4 $\mu\text{A}$
ADC Sampling	0.3 $\mu\text{A}$
Software Processing	3.0 $\mu\text{A}$
<b>TOTAL</b>	<b>8.1 <math>\mu\text{A}</math></b>

## 5.2 Ambient Light Sensing

### 5.2.1 Accuracy

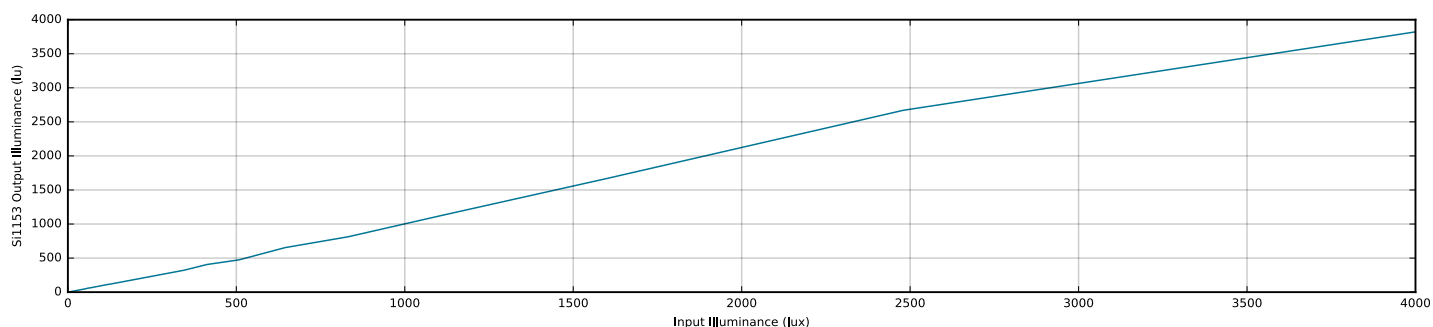
The accuracy of the Si1153 ambient light sensor was measured by comparing the output of the system with a calibrated ILT1400 radiometer with SCL110 illuminance attachment.

The illuminance was varied by modifying the source-detector distance. The detectors were aligned in the center of the optical field at normal-angle incident of light. The source was a white LED bulb.

The error here is defined as the error between the Si1153 and the SCL110 detector head, when they are positioned to the same location within the light field. The tests were performed on an optical rail for distance repeatability and aligned to the optical center of the light field. The test environment was blocked from ambient light to avoid interference.

Parameter	Condition	Measured
Error	White LED	$\pm 25\%$

Figure 5.2. Si1153 Output Illuminance vs Input Illuminance



### 5.2.2 Power Measurement

The current consumption of the system was measured using the Advanced Energy Monitoring (AEM) tool included in the Starter Kit hardware and Simplicity Studio. This tool allows for real time monitoring of current consumption with 0.1  $\mu\text{A}$  resolution at 6.3 ksps. Average current was measured over 30 s to account for the pulsed nature of the software. All current consumption through the VMCU power rail is measured which includes the MCU, sensor and I2C communication.

The sensor is operated at 1 sample per second output rate triggered by the RTC.

Block	Current Consumption
EFM32 MCU EM2	3.4 $\mu\text{A}$
RTC 1 Hz	0.5 $\mu\text{A}$
Si1153 Ambient Light Sensing	28.5 $\mu\text{A}$
<b>TOTAL</b>	32.4 $\mu\text{A}$



## 6. Hardware Details

### 6.1 Schematics

To download the schematic files, see the Evaluation Kit Resources for the OCCUPANCY-EXP-EVB on <https://www.silabs.com> or look up OCCUPANCY-EXP-EVB in Simplicity Studio.

### 6.2 Bill of Materials

To download the bill of materials (BOM), see the Evaluation Kit Resources for the OCCUPANCY-EXP-EVB on <https://www.silabs.com> or look up OCCUPANCY-EXP-EVB in Simplicity Studio.

### 6.3 Assembly Drawings

To download the assembly drawings, see the Evaluation Kit Resources for the OCCUPANCY-EXP-EVB on <https://www.silabs.com> or look up OCCUPANCY-EXP-EVB in Simplicity Studio.

### 6.4 Gerber Files

To download the bill of materials (BOM), see the Evaluation Kit Resources for the OCCUPANCY-EXP-EVB on <https://www.silabs.com> or look up OCCUPANCY-EXP-EVB in Simplicity Studio.

## 6.5 Expansion Header

On the left-hand side of the board, an angled 20 pin expansion header is provided to connect with Silicon Labs' MCU starter kits. The figure below shows the pin assignment of the expansion header for the OCCUPANCY-EXP-EVB kit. The diagram is oriented when the connector is viewed from the top of the board.

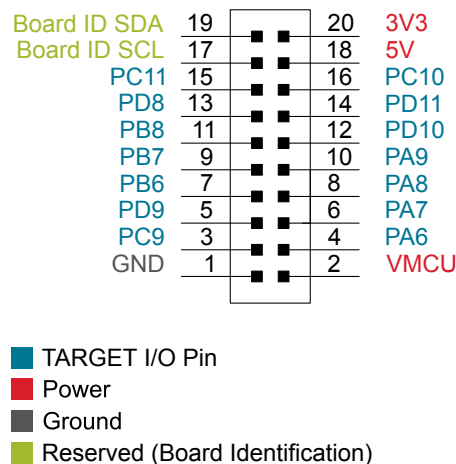


**Figure 6.1. Expansion Header**

**Table 6.1. EXP Header Pin out**

Pin	Connection	EXP Kit Function	Peripheral Mapping
20	3V3	Board controller supply	
18	5V	Board USB voltage	
16	PC10	SENSOR_SDA	I2C0.SDA
14	PD11	SENSOR_INT	
12	PD10	MOTION_B	
10	PA9		
8	PA8		
6	PA7		
4	PA6	ADC_N	ADC0 adcNegSel4YCH14
2	VMCU	EFM32 and sensor voltage domain, included in AEM measurements.	
19	BOARD_ID_SDA	Connected to MCU starter kit for identification of expansion board.	
17	BOARD_ID_SCL	Connected to MCU starter kit for identification of expansion board.	
15	PC11	SENSOR_SCL	I2C0.SCL
13	PD8	LDO_SHDN_B	
11	PB8		
9	PB7		
7	PB6		
5	PD9		

Pin	Connection	EXP Kit Function	Peripheral Mapping
3	PC9	ADC_P	ADC0 adcPosSel2XCH9
1	GND	Ground	

## 7. Software Details

### 7.1 Importing the Firmware Example

This section describes how to import the OccupancySensorExp example code into Simplicity Studio™ and run it on a SLSTK3402A EFM32PG12 Starter Kit. The project requires Simplicity Studio v4. Simplicity Studio can be downloaded at <https://www.silabs.com/products/development-tools/software/simplicity-studio>.

1. Download source code from <https://github.com/SiliconLabs/occupancy-sensor-exp>. A zip file can be downloaded using the 'Clone or download' button and selecting Download ZIP.
2. In Simplicity Studio, click on File → Import Project
3. Click on More Import Options at the bottom left corner.
4. Choose Existing Projects into Workspace as the import source. Click Next.
5. Navigate to where you downloaded the source code to select the root directory. Select the OccupancySensorExp project and click Finish.
6. Compile by right clicking on the project in the Project Explorer and selecting Build Project.
7. Download the project to the MCU by right clicking on the project in the Project Explorer and selecting Run As → Silicon Labs ARM Project.

## 7.2 PIR GUI Details

The PIR GUI provides a convenient way to visualize PIR signals in real time so that motion signals can be captured and parameters optimized. The PIR GUI displays the ADC output, detector thresholds, and motion output from the firmware example code. Captured data can be exported for future analysis and imported for later viewing.

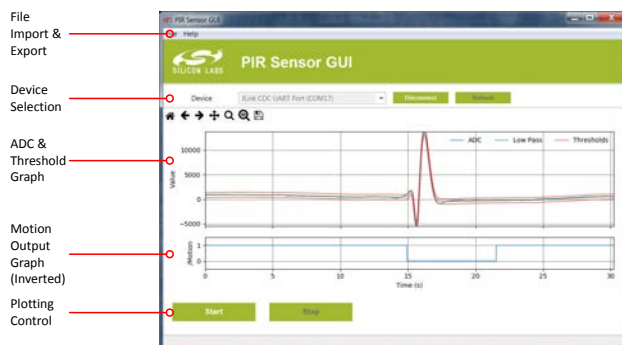


Figure 7.1. PIR GUI User Interface

The PIR GUI only requires a few steps to get up and running.

- Install the PIR GUI. The software can be downloaded from the Evaluation Kit resources for OCCUPANCY-EXP-EVB on <https://www.silabs.com>.
- Run the firmware demo from Simplicity Studio. Start the PIR demo using BTN0 on the STK board. Do not use the PIR LCD OFF demo as it disables the COM port communication low power current measurements.
- Connect the GUI to the COM port using the Device Selection panel. The description should say JLink CDC UART Port.
- Press Start. The ADC and motion waveforms should appear on the graphs.

### Features

#### • Zooming

By default, the graph shows the last 30 seconds of captured data. This can be toggled using the Zoom Recent/All tool in the toolbar. Additional selectable zooming can be performed using the Zoom and Pan tools.

#### • Data Import / Export

Images of the graphs can be saved using the Save icon in the toolbar above the graphs. Data import and export is available through the File menu. The data is read/written to CSV with following format.

```
time, adc, motionb, winbase, adcThreshHigh, adcThreshLow
```

time: Time since capture began in seconds.

adc: ADC differential output. int16\_t.

motionb: Motion output of the detector. Active low. bool

winbase: Window center of the detector in ADC codes. int16\_t.

adcThreshHigh: Upper threshold of the detector in ADC codes. int16\_t

adcThreshLow: Lower threshold of the detector in ADC codes. int16\_t

## 8. Kit Revision History and Errata

### 8.1 Revision History

The kit revision can be found printed on the evaluation board, as outlined in the figure below.

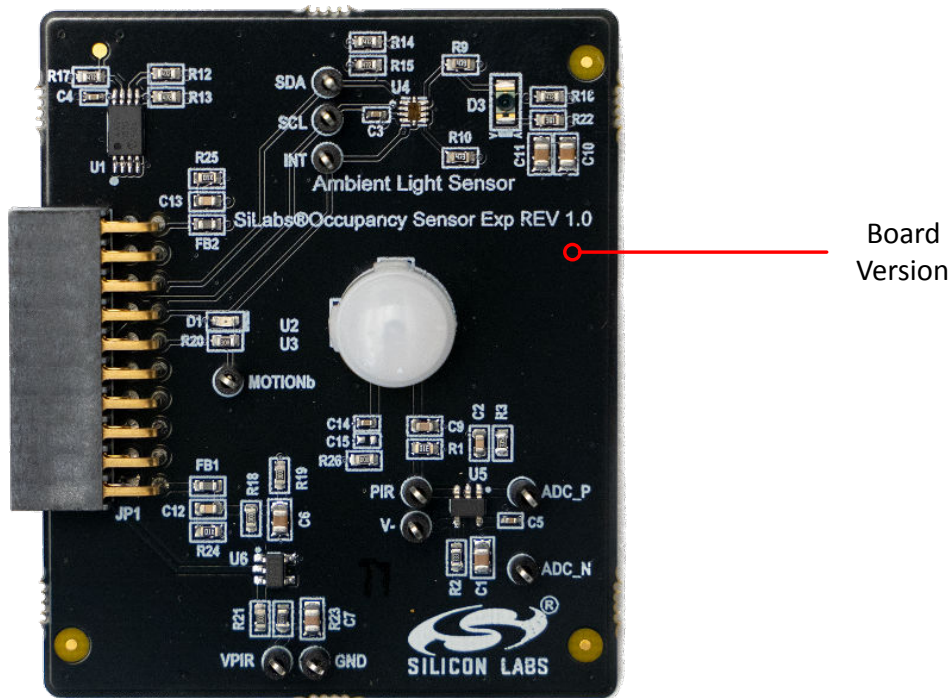


Figure 8.1. Kit Revision History

Kit Revision	Released	Description
1.0	2019-02-13	Initial kit release

### 8.2 Errata

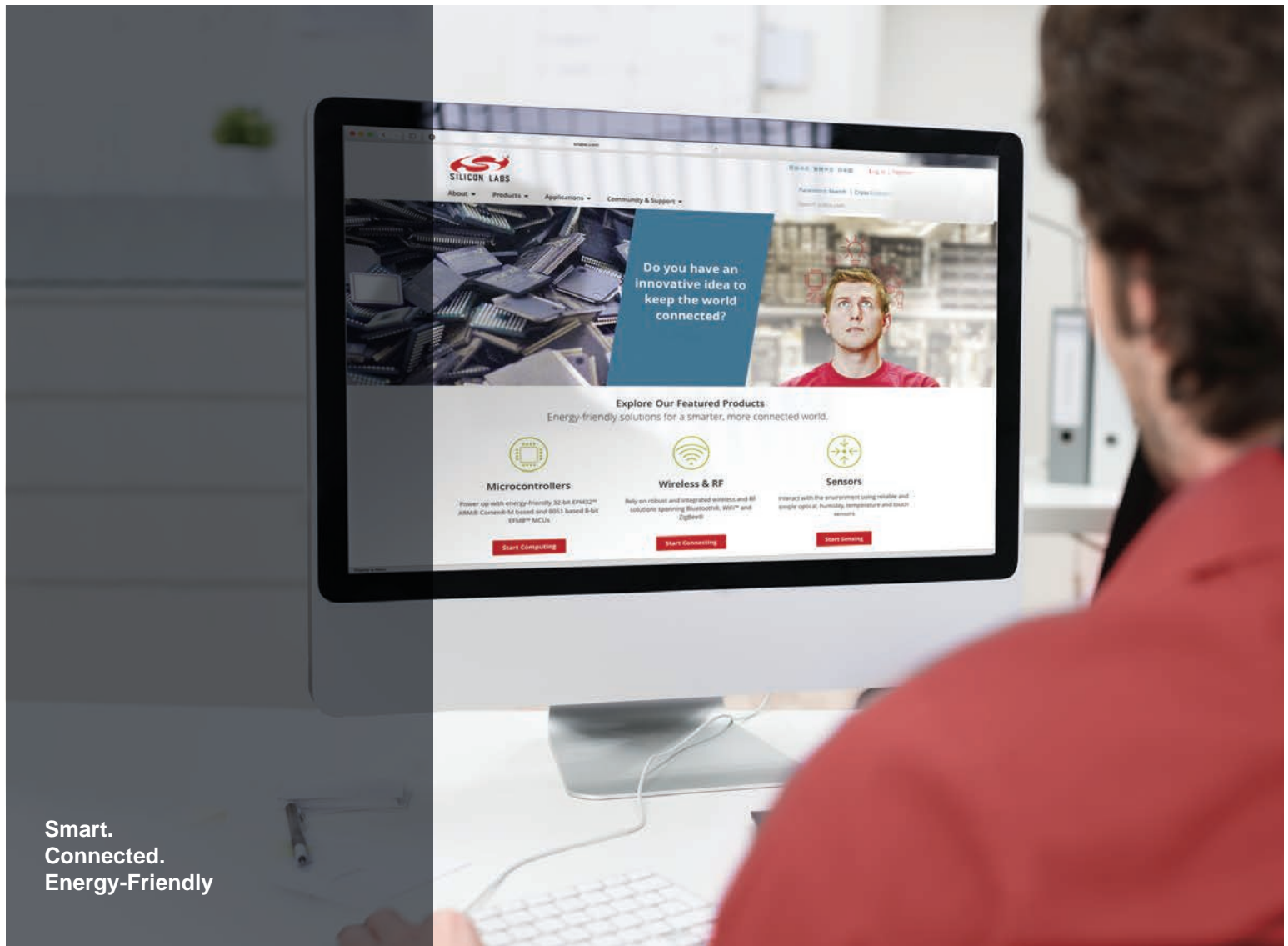
There are no known errata at present.

## 9. Revision History

### Revision 1.0

February 13, 2019

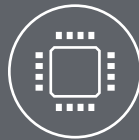
- Initial release.



Smart.  
Connected.  
Energy-Friendly



**Products**  
[www.silabs.com/products](http://www.silabs.com/products)



**Quality**  
[www.silabs.com/quality](http://www.silabs.com/quality)



**Support and Community**  
[community.silabs.com](http://community.silabs.com)

#### Disclaimer

Silicon Labs intends to provide customers with the latest, accurate, and in-depth documentation of all peripherals and modules available for system and software implementers using or intending to use the Silicon Labs products. Characterization data, available modules and peripherals, memory sizes and memory addresses refer to each specific device, and "Typical" parameters provided can and do vary in different applications. Application examples described herein are for illustrative purposes only. Silicon Labs reserves the right to make changes without further notice to the product information, specifications, and descriptions herein, and does not give warranties as to the accuracy or completeness of the included information. Without prior notification, Silicon Labs may update product firmware during the manufacturing process for security or reliability reasons. Such changes will not alter the specifications or the performance of the product. Silicon Labs shall have no liability for the consequences of use of the information supplied in this document. This document does not imply or expressly grant any license to design or fabricate any integrated circuits. The products are not designed or authorized to be used within any FDA Class III devices, applications for which FDA premarket approval is required or Life Support Systems without the specific written consent of Silicon Labs. A "Life Support System" is any product or system intended to support or sustain life and/or health, which, if it fails, can be reasonably expected to result in significant personal injury or death. Silicon Labs products are not designed or authorized for military applications. Silicon Labs products shall under no circumstances be used in weapons of mass destruction including (but not limited to) nuclear, biological or chemical weapons, or missiles capable of delivering such weapons. Silicon Labs disclaims all express and implied warranties and shall not be responsible or liable for any injuries or damages related to use of a Silicon Labs product in such unauthorized applications.

#### Trademark Information

Silicon Laboratories Inc.®, Silicon Laboratories®, Silicon Labs®, SiLabs® and the Silicon Labs logo®, Bluegiga®, Bluegiga Logo®, Clockbuilder®, CMEMS®, DSPLL®, EFM®, EFM32®, EFR®, Ember®, Energy Micro, Energy Micro logo and combinations thereof, "the world's most energy friendly microcontrollers", Ember®, EZLink®, EZRadio®, EZRadioPRO®, Gecko®, ISOModem®, Precision32®, ProSLIC®, Simplicity Studio®, SiPHY®, Telegesis, the Telegesis Logo®, USBXpress® and others are trademarks or registered trademarks of Silicon Labs. ARM, CORTEX, Cortex-M3 and THUMB are trademarks or registered trademarks of ARM Holdings. Keil is a registered trademark of ARM Limited. All other products or brand names mentioned herein are trademarks of their respective holders.



Silicon Laboratories Inc.  
400 West Cesar Chavez  
Austin, TX 78701  
USA

<http://www.silabs.com>



# Mouser Electronics

Authorized Distributor

Click to View Pricing, Inventory, Delivery & Lifecycle Information:

[Silicon Laboratories:](#)

[Occupancy-EXP-EVB](#)